Disorder-induced decoupling of attracting identical fermions: Transfer matrix approach

Lolita I. Knyazeva [1,2,*] and Vladimir I. Yudson [3,1,†]
[1]*Russian Quantum Center, Skolkovo, Moscow 143025, Russia*
[2]*Moscow Institute of Physics and Technology, Dolgoprudny 141700, Russia*
[3]*Laboratory for Condensed Matter Physics, HSE University, Moscow 101000, Russia*

(Received 5 November 2023; revised 15 December 2023; accepted 19 December 2023; published 8 January 2024)

We consider a pair of identical fermions with a short-range attractive interaction on a finite lattice cluster in the presence of strong site disorder. This toy model imitates a low-density regime of the strongly disordered Hubbard model. In contrast to spinful fermions, which can simultaneously occupy a site with minimal energy and thus always form a bound state resistant to disorder, for the identical fermions the probability of pairing on neighboring sites depends on the relation between the interaction and the disorder. The complexity of "brute-force" calculations (both analytical and numerical) of this probability grows rapidly with the number of sites even for the simplest cluster geometry in the form of a closed chain. Remarkably, this problem is related to the old mathematical task of computing the volume of a polyhedron, known as NP-hard. However, we have found that the problem in the chain geometry can be exactly solved by the transfer matrix method. Using this approach, we have calculated the pairing probability in the long chain for an arbitrary relation between the interaction and the disorder strengths and completely describe the crossover between the regimes of coupled and separated fermions.

DOI: 10.1103/PhysRevB.109.024202

I. INTRODUCTION

The interplay of disorder and interaction is one of the central problems of condensed matter physics. It gives rise to a plethora of fundamental phenomena, including metal-insulator and superconductor-insulator transitions, "bad metals," and spin and electron glasses, to mention just few [1–6]. Recently, some of these traditionally condensed matter topics have also become a subject of interest in systems of ultracold atoms in optical traps [7,8].

A paradigmatic platform to study these phenomena in a quantum ensemble of interacting particles is the seminal Hubbard model [9] with its very rich and complicated physics. In this paper we consider a simplified version of this model for identical fermions with a short-range attractive interaction in the limiting regime of low density and strong site disorder. Assuming the intersite hopping parameter is small compared to both the interaction and the disorder, we get a system where the quantumness of particles is suppressed (except for the fermionic statistics), and they may be considered to be located on different lattice sites [10]. Finding the ground state and correlation functions for this kind of electron glass reduces to a statistical, but still rather complicated, problem. The particles can form clusters whose size distribution is determined by the relative strength of the interaction and the disorder.

Here, as the first step towards the solution of the many-particle problem, we study a toy model of just two identical fermions restricted to a finite strongly disordered lattice with N sites, so $2/N$ is an effective fermion "density" (filling factor). The quantity of interest is the probability P_b of forming the "bound pair" of fermions due to their attractive nearest-neighbor interaction. In the case of nonidentical fermions with an attractive on-site interaction, the model would be trivial: two fermions occupy a site with minimal energy and thus always form a bound state. But identical fermions should occupy different sites, and if the disorder is stronger than the interaction, it may happen that the fermions located on neighboring sites have higher energy than those located on some separated (non-neighboring) sites.

The probability to find two neighboring sites for which the energy of the attracting fermions is minimal increases with the increase of the system size. Therefore, such particles in an infinite system necessarily form a bound state despite the presence of the disorder. However, in a finite-size cluster the problem of an energetically advantageous arrangement of two attracting fermions on neighboring or on distant sites becomes quite challenging. The probability P_b should be calculated as a function of N and of the interaction and disorder strengths. Moreover, it depends on the connectivity of the lattice. For simplicity, keeping in mind the possibility of an exact analytical approach, we restrict our analysis to the one-dimensional case and consider a system in the form of a closed N-site chain.

The condition that the bound state corresponds to the minimal energy is represented by a set of ($\propto N^2$) linear inequalities for random potentials on the system sites, and the probability P_b is determined by the averaging of these inequalities over the realization of the disorder. Remarkably, with the simplest, boxlike distribution of the disorder this problem is equivalent to the calculation of the volume of a domain (polyhedron) in the N cube restricted by a set of ($\propto N^2$) hypersurfaces. This problem is known to be NP-hard: owing to the rapidly

*kniazeva.li@phystech.edu
†vyudson@hse.ru

(perhaps, faster than exponentially in N) growing complexity of the system, the possibility of straightforward brute-force calculations, both analytical and numerical, is practically restricted to small N.

Nevertheless, somewhat surprisingly for a disordered system [11], it turns out that the considered problem in the chain geometry allows for the transfer matrix approach. The eigenstates and eigenvalues of this transfer matrix obey an intricate integral equation. Another surprise is that this integral equation turns out to be solvable analytically. Implementing this approach, we have calculated the pairing probability P_b in the large-N limit for an arbitrary relation between the interaction and the disorder strengths.

In Sec. II we describe the model and formulate a set of conditions imposed on the random potentials to yield the existence of the bound state. Section II also illustrates the exact brute-force approach in the simplest nontrivial case, a chain with $N = 4$ sites, and describes problems of extending this approach to higher N. In Sec. III we present the results of numerical (stochastic) experiments and quantitatively interpret them for the weak interaction case. In Sec. IV we develop the transfer matrix approach and calculate the probability P_b in the large-N limit for an arbitrary relation between the interaction and the disorder strengths. In Sec. V we summarize the obtained results and discuss possible issues for future research.

II. THE MODEL

We consider a pair of identical fermions in a finite lattice cluster described by the Hubbard model [9] with the nearest-neighbor attractive interaction $\widetilde{U}$. The short-range hopping amplitude is assumed to be much smaller than both $\widetilde{U}$ and the disorder distribution width W. Thus, the hopping has an almost negligible influence on the ground state of the strongly disordered system and can be ignored. The aim of our work is to find the probability P_b that two fermions in the ground state are "bound," i.e., occupy two neighboring sites. In an infinite cluster with the number of sites $N \to \infty$ the probability $P_\mathrm{b} \to 1$ for any nonzero $\widetilde{U}$, while in a finite cluster it depends on relations between the parameters $\widetilde{U}$, W, and N, as well as on the geometry (connectivity matrix) of the cluster. Calculation of P_b as a function of these parameters is a quite nontrivial problem. Here, we restrict our analysis to the simplest cluster in the form of a closed chain, where the solution can be obtained by the transfer matrix method. For the random on-site potentials $\widetilde{V}_i$ we choose the box probability distribution $p(\widetilde{V}_i) = \theta(W - \widetilde{V}_i)\theta(\widetilde{V}_i)/W$, although some of the derived expressions hold for a generic bell-shaped distribution. The system Hamiltonian can be presented in the dimensionless form

$$H = \sum_{i=1}^{N} V_i n_i - U \sum_{i=1}^{N} n_i n_{i+1}, \tag{1}$$

where n_i is the number of fermions (one or zero fermions) on site i and the total number of fermions on the chain equals two. The interaction constant and the random potentials are measured in units of the disorder distribution width W: $U = \widetilde{U}/W$ and $V_i = \widetilde{V}_i/W$, so the disorder box-distribution function takes the form

$$p(V_i) = \theta(V_i)\theta(1 - V_i). \tag{2}$$

For a given disorder realization, the condition that the ground state of the two-fermion system corresponds to the fermions located on some neighboring sites (say, i and $i+1$) means that the energy $V_i + V_{i+1} - U$ is less than energies of all other arrangements of fermions. If $U \geqslant 1$, this condition of forming the bound state is fulfilled for any realization of disorder, so $P_b(U \geqslant 1) = 1$. Indeed, if the site i corresponds to the minimal (in the given realization) potential V_i, then the energy $V_i + V_{i\pm1} - U < V_j + V_l$ for any pair (j, l) of non-neighboring sites, as $V_i < V_j$ and $V_{i\pm1} - U < 0 < V_l$.

In the other limiting case, $U = 0$, the noninteracting fermions occupy two sites with minimal potentials. As the random potentials on different sites are distributed independently, the probability for two fermions to occupy neighboring sites is simply given by the ratio of the number N of such arrangements (in the considered ring geometry) to the total number C_N^2 of possible arrangements:

$$P_b(U = 0) = 2/(N - 1). \tag{3}$$

For brevity, we will refer to the fermion pair located on neighboring sites as the "bound pair" even at $U = 0$, although the quantity (3) is purely combinatoric. Note that $P_b(U = 0) \to 0$ when $N \to \infty$.

Our task is to find $P_b(U)$ in the interval $0 < U < 1$. Due to the symmetry of the considered ring cluster, the probability $P_\mathrm{b} = NP_{12}^\mathrm{b}$, where P_{12}^b is the probability that the first and second sites are occupied, i.e., the energy $V_1 + V_2 - U$ is lower than the energies of all other arrangements. This requirement is provided by a set of inequalities:

$$V_1 + V_2 - U < V_j + V_l, \;\; j = \overline{2, N-2}, \;\; l = \overline{j+2, N}; \tag{4}$$

$$V_2 - U < V_l, \;\; l = \overline{3, N-1}; \tag{5}$$

$$V_1 + V_2 < V_j + V_{j+1}, \;\; j = \overline{2, N-1}; \quad V_2 < V_N, \tag{6}$$

where the overlines indicate the intervals for site numbers j and l. Inequalities (4) and (5) mean that the energy of the fermion pair on sites 1 and 2 is lower than that for fermions occupying non-neighboring sites. Inequalities (6) ensure that the selected pair of sites (1,2) provides lower energy compared to that for other neighboring arrangements. The probability $P_b(U)$ is determined by the averaging of the above conditions over the realizations of the random potentials:

$$\begin{aligned} P_b(U) = N\Big\langle & \theta(V_N - V_2) \prod_{j=2}^{N-1} \theta(V_j + V_{j+1} - V_1 - V_2) \\ & \times \prod_{j=2}^{N-2} \prod_{l=j+2}^{N} \theta(V_j + V_l - V_1 - V_2 + U) \\ & \times \prod_{l=3}^{N-1} \theta(V_l - V_2 + U) \Big\rangle. \end{aligned} \tag{7}$$

Here, $\langle \cdots \rangle$ means the averaging over the disorder. For the box distribution (2), this means multiple integrals over the unit

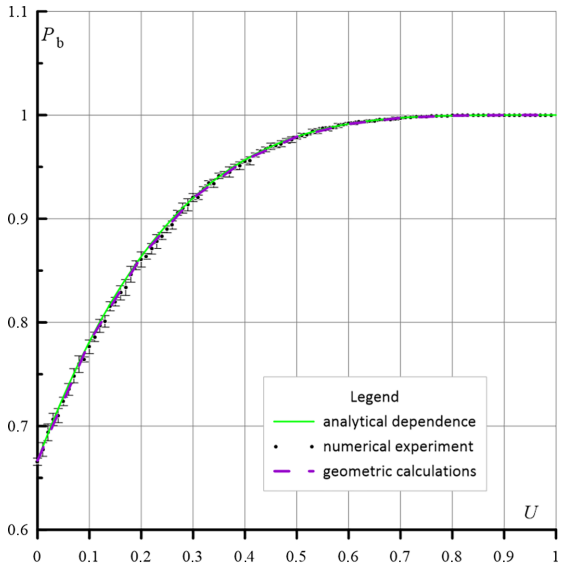

FIG. 1. Dependence of the probability to observe a bound state P_b on the interaction U (in units of the disorder width) for the number of sites $N = 4$.

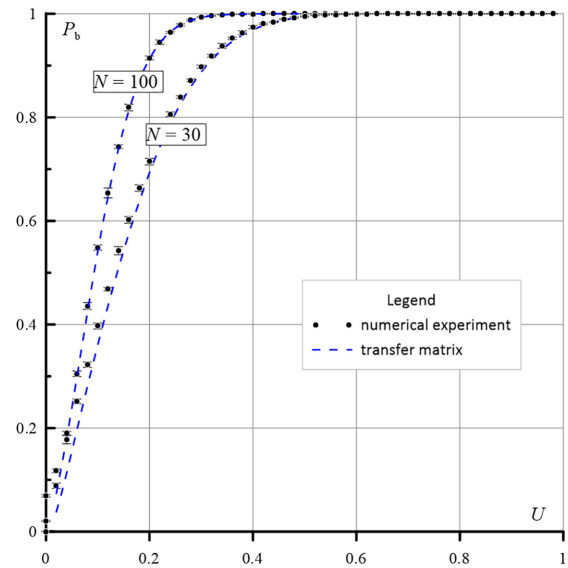

FIG. 2. Crossover between the coupling and decoupling regimes. Dependences of the probability P_b on the interaction U calculated in the numerical experiments for the number of sites $N = 30$ and $N = 100$ are presented.

N-dimensional hypercube. The θ functions in the integrand yield conditions (4)–(6).

Being linear in random potentials, these conditions correspond to a set of hyperplanes restricting the integration domain to a very intricate N-dimensional polyhedron. Finding the exact volume of a polyhedron is an old mathematical problem; computing this volume is NP-hard (see, e.g., [12,13] and references therein). Also, the direct analytical integration is highly repetitive and tedious. For the particular integral (7), *a priori* we can say only that it determines a polynomial function of the Nth order in U that obeys (3) and tends to unity when $U \to 1$. To illustrate the situation we consider the simplest case $N = 4$, where the integral (7) can still be easily calculated.

A. The simplest nontrivial case, $N = 4$

The ring of ($N = 4$) sites is the shortest one in which not all sites are neighboring. Using conditions (4)–(6), we can represent P_b (7) in the form

$$P_b = 4 \int p(V_1)p(V_2)f(V_1, V_2)f(V_2, V_1)dV_1dV_2, \qquad (8)$$

where

$$f(V_1, V_2) = \int \theta(V_3 - V_2 + U)\theta(V_3 - V_1)p(V_3)dV_3,$$

$$f(V_2, V_1) = \int \theta(V_4 - V_1 + U)\theta(V_4 - V_2)p(V_4)dV_4. \qquad (9)$$

These expressions are valid for any distribution of random potentials. Substituting the uniform distribution (2), we obtain $P_b = 4P_{12}^b$

$$P_b = 1 - \tfrac{1}{3}(1 - U)^4. \qquad (10)$$

In Fig. 1 we see that this analytical dependence coincides with the results of a direct numerical calculation of the integral as well as with the numerical (Monte Carlo) experiment. Even this simple example demonstrates the basic features of the effect: attracting fermions on a finite lattice (ring) are coupled in the case of a relatively weak disorder ($U = \widetilde{U}/W > 1$), but they can be decoupled in the case of a relatively strong disorder ($U = \widetilde{U}/W < 1$); if the disorder is very strong ($U = \widetilde{U}/W \ll 1$), the fermions are arranged almost independently.

III. NUMERICAL RESULTS AND QUALITATIVE ANALYSIS

The crossover between the coupling and decoupling regimes depends on the cluster size (ring length N); see the dot results for the numerical (Monte Carlo) experiment in Fig. 2. However, a description of these results by the brute-force analytical or numerical calculations can hardly be achieved for a high N: with the increase of the number of sites N, the time required for calculations grows very rapidly (see Table I).

To gain more insight into the problem, we will develop physical approaches and verify them with the results of numerical experiments. The numerical experiments have been performed as a search for the minimal energy in a particular realization of disorder. Counting the cases in which the minimal energy corresponds to fermions occupying neighboring

TABLE I. The time required to calculate the volume of a polyhedron in N-dimensional space that determines the probability of formation of a bound pair of identical fermions in a closed chain of N sites. The results for interaction value $U = 0.2$ are presented.

	N			
	4	5	6	7
Time (s)	3.407	32.500	632.812	13273.593

sites, we have calculated the probability of a bound state using 10 000 realizations of the disorder.

We begin with the analysis of the weak interaction case $U \ll 1$.

A. Weak interaction

To warm up, consider a linear in $U \ll 1$ correction to $P_b(U=0)$ [Eq. (3)]. First, let us show how the latter follows from the general expression (7) due to the inequalities (5): in the noninteracting case they reduce to $V_l > \max\{V_1, V_2\}$ for $l \in (3, \ldots, N)$, so the multiple integral (7) takes the form

$$P_b(0) = 2N \int dV_1 p(V_1) \int dV_2 \theta(V_2 - V_1) p(V_2) \times \left[\int \theta(V - V_2) p(V) dV \right]^{N-2}. \quad (11)$$

Here, the integration goes over the sector $V_1 < V_2$, while the contribution of the sector $V_2 < V_1$ is accounted for by the factor of 2 before the integral. Twice applying the relation

$$p(V) \left[\int \theta(V' - V) p(V') dV' \right]^M = -\frac{1}{M+1} \frac{d}{dV} \left[\int \theta(V' - V) p(V') dV' \right]^{M+1}, \quad (12)$$

we arrive at Eq. (3). Naturally, this combinatoric result holds for an arbitrary distribution function $p(V)$. To find the linear in U correction $P_b^{(\mathrm{lin})}$ to Eq. (3) one should sequentially expand the θ functions in the integrand of Eq. (7), $\theta(V+U) \to \theta(V) + U\delta(V)$. Summing up the contributions from all θ functions, we obtain $P_b^{(\mathrm{lin})}(U)$ in the following form:

$$P_b^{(\mathrm{lin})}(U) = 2N(N-3)U \int dV_1 p(V_1) \int dV_2 \theta(V_2 - V_1) \times p^2(V_2) \left[\int dV \theta(V_2 - V) \right]^{N-3}. \quad (13)$$

Because of the δ function, the probability distribution for one of the sites is squared, and quite expectably, the integral depends on the explicit shape of the distribution. For the considered box distribution (2) we obtain

$$P_b^{(\mathrm{lin})}(U) = \frac{2N(N-3)}{(N-2)(N-1)} U. \quad (14)$$

The coefficient of U tends to 2 for large N.

Putting the obtained linear dependences (14) in the results of the numerical experiment (Fig. 3), we observe that the linear asymptotics are true in the region $U \ll 1/N$ but deviate from the experiment at $1/N \leqslant U$.

B. Crossover

A wider range of the interaction strength $1/N \ll U \ll 1$ can be described with the following reasoning. The average energy distance between N on-site potentials, randomly distributed over the unit energy interval, is $1/N$. An average number of sites with random potentials $V < \eta U$, where $\eta \lesssim 1$, is given by $K = \eta U N$ and obeys the inequality $1 \ll K \ll N$. If two such sites are neighboring, the fermion pair located on them will certainly (for $\eta < 1/2$) or with good probability (if $1/2 < \eta \lesssim 1$) have a negative energy; that is, it will be bound. The probability P_b that a fermion pair is bound can be represented as $P_b = 1 - P_s$, where P_s is the probability that the two fermions are separated, that is, among the K sites there are no neighboring ones. This elementary combinatorial problem gives (in the limit $1 \ll K \ll N$) $P_s = \exp(-K^2/N)$. Combining with Eqs. (3) and (14), we arrive at the interpolation formula for $P_b(U)$ at $U \ll 1$:

$$P_b(U) \approx \frac{2}{N} + 2U + 1 - e^{-\eta^2 N U^2} \approx \eta^2 N U^2, \quad (15)$$

where the last equality corresponds to the narrower intermediate interval $1/N \ll U \ll 1\sqrt{N}$ and shows the dominant quadratic dependence of the function $P_b(U)$ on U presented in Fig. 3. Although the numerical constant $\eta \lesssim 1$ still remains uncertain (it will be fixed in Sec. IV), Eq. (15) allows us to infer that the crossover between the regimes of almost decoupled and almost coupled fermions occurs at $U \sim 1/\sqrt{N}$. These behaviors agree with the numerical experiment (dots in Fig. 2).

We note in passing that the above qualitative analysis of the crossover can be extended to a cluster of arbitrary dimension d, resulting in the expression $P_s = \exp(-d\eta^2 U^2 N)$. This allows us to conjecture that the estimate $U \sim 1/\sqrt{N}$ for the crossover range is universal. A regular description of the crossover will be developed below for the one-dimensional cluster (chain) using the transfer matrix approach.

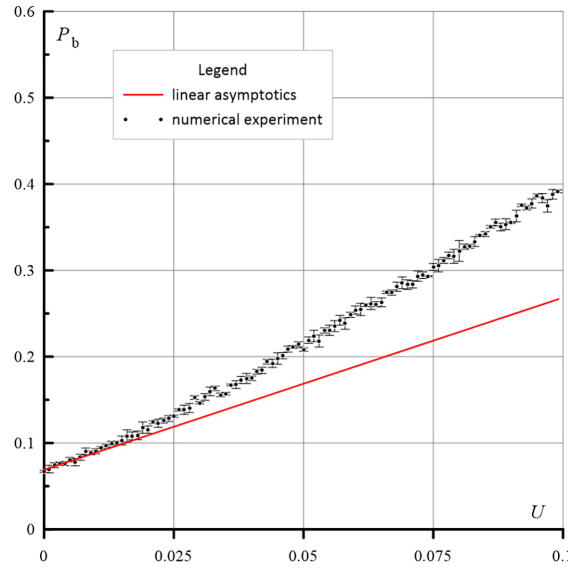

FIG. 3. Dependence of the bound state probability $P_b(U)$ on the relative interaction strength U in the range of $U \ll 1$ for the number of sites $N = 30$.

IV. TRANSFER MATRIX METHOD

A. Basic equations

Consider the case where the ground state corresponds to separated fermions, i.e., occupying two non-neighboring sites, e.g., the first and the kth ones ($k \neq 2, N$). Due to the equivalence of configurations $(1, k)$, $(2, k+1)$, etc., the

probability $P_s(1,k)$ of this particular arrangement is simply connected to the total probability $P_s = 1 - P_b$ of the realization of separated fermions:

$$P_s = \frac{N}{2}\sum_{k=3}^{N-1} P_s(1,k). \tag{16}$$

To correspond to the ground state, the energy of the configuration with fermions located on the first and kth sites, $V_1 + V_k$, should obey a set of obvious inequalities, such as $V_1 + V_k < V_i + V_{i+1} - U$, $V_1 + V_k < V_i + V_k$ $(i \neq 1, k-1, k, k+1)$, etc. The probability $P_s(1,k)$ is determined by averaging these inequalities over the disorder:

$$P_s(1,k)(U) = \Big\langle \theta(V_N - \varepsilon_1) \prod_{i=k+1}^{N-1} [\theta(V_{i+1} - \varepsilon)\theta(V_{i+1} + V_i - U - E)\theta(V_i - \varepsilon)]\, \theta(V_{k+1} - \varepsilon_k)$$
$$\times\, \theta(V_{k-1} - \varepsilon_k) \prod_{i=2}^{k-2} [\theta(V_{i+1} - \varepsilon)\theta(V_{i+1} + V_i - U - E)\theta(V_i - \varepsilon)]\, \theta(V_2 - \varepsilon_1) \Big\rangle. \tag{17}$$

Here, we have introduced several parameters, ε_1, ε_k, E, and ε, determined by the potentials V_1 and V_k:

$$\varepsilon_1 = \max\{V_1, V_k + U\}, \quad \varepsilon_k = \max\{V_k, V_1 + U\},$$
$$E = V_1 + V_k, \quad \varepsilon = \max\{V_1, V_k\}. \tag{18}$$

Expression (17) is represented in a form suitable for the celebrated transfer matrix approach [14]. For this aim we introduce the operator $\hat{A}$

$$\hat{A}(V, V') = \sqrt{p(V)}\,\theta(V - \varepsilon)\theta(V + V' - U - E)$$
$$\times\, \theta(V' - \varepsilon)\sqrt{p(V')} \tag{19}$$

and note that the matrix product

$$\hat{A}^2(V, V') = \int \hat{A}(V, V'')\hat{A}(V'', V')dV'' \tag{20}$$

just corresponds to the product of two subsequent blocks in Eq. (17) with averaging over the intermediate variable, i.e., with integration with weight $p(V'')$. Thus, $\hat{A}(V_{i+1}, V_i)$ is the desired transfer matrix between sites i and $i+1$ for a chain with an arbitrary disorder distribution function $p(V)$. Postponing the study of this general case to the future, in the present paper we concentrate on the particular case of the box distribution (2), so

$$\hat{A}(V, V') = \theta(V - \varepsilon)\theta(V + V' - U - E)\theta(V' - \varepsilon). \tag{21}$$

Note that $\hat{A}$ depends on the parameters E and ε, determined entirely by the potentials on the two selected sites [see Eq. (18)].

Using Eqs. (20) and (21), the probability (17) can be rewritten in the form

$$P_s(1,k) = \langle \theta(V_N - \varepsilon_1)\hat{A}^{N-k-1}(V_N, V_{k+1})\theta(V_{k+1} - \varepsilon_k)$$
$$\times\, \theta(V_{k-1} - \varepsilon_k)\hat{A}^{k-3}(V_{k-1}, V_2)\theta(V_2 - \varepsilon_1)\rangle. \tag{22}$$

Here, the first and second lines result from the integration over $V_{N-1}, \ldots, V_{k+2}$ and $V_{k-2}, \ldots, V_3$, respectively. The remaining averaging over the disorder is reduced to integration over the potentials on the first and kth sites and on their nearest neighbors.

Being real and symmetric in V and V', the transfer matrix $\hat{A}$ can be represented as

$$\hat{A}(V, V') = \sum_\nu \varphi_\nu(V)\lambda_\nu\varphi_\nu(V'), \tag{23}$$

where the eigenfunctions $\varphi_\nu(V)$ obey the equation $\hat{A}\varphi_\nu = \lambda_\nu\varphi_\nu$ and constitute an orthonormal basis. Like the matrix $\hat{A}$, the eigenfunctions and the eigenvalues depend on the "external" parameters E and ε. Powers of $\hat{A}$ are given by

$$\hat{A}^M(V, V') = \sum_\nu \varphi_\nu(V)\lambda_\nu^M\varphi_\nu(V'). \tag{24}$$

For large M the leading term in the sum (24) is that with the largest modulus eigenvalue, say, λ_0. The central point of the transfer matrix method is to replace $\hat{A}^M$ by its leading part:

$$\hat{A}^M(V, V') \to \varphi_0(V)\lambda_0^M\varphi_0(V'). \tag{25}$$

In our case of a long chain, the leading contribution to the sum (16) is provided by sites with $k \sim N \gg 1$, so the transfer-matrix method is appropriate. Applying Eq. (25) to Eq. (22), we see that in this limit the contribution of a particular pair of sites [like $(1,k)$] does not depend on k. Therefore, in the leading order in N we obtain

$$P_s = \frac{N^2}{2}\int_0^1\int_0^1 dV_1 dV_k \lambda_0^{N-4} I^2(\varepsilon_1) I^2(\varepsilon_k), \tag{26}$$

where the function $I(e)$ is defined by

$$I(e) = \theta(1 - e)\int_e^1 \varphi_0(V)dV. \tag{27}$$

The integrand in Eq. (26) is an implicit function of the variables V_1 and V_k [see Eq. (18)], subject to the constraints imposed by Eq. (27):

$$\varepsilon_1,\ \varepsilon_k < 1 \ \Rightarrow\ V_1, \quad V_k < 1 - U. \tag{28}$$

To proceed we need to find the largest eigenvalue λ_0 and the corresponding eigenfunction $\varphi_0(V)$.

B. Solution of the integral equation $\hat{A}\varphi_\nu = \lambda_\nu\varphi_\nu$

In accordance with Eq. (21), the integral equation

$$\int_0^1 \hat{A}(V, V')\varphi(V')dV' = \lambda\varphi(V) \tag{29}$$

is actually restricted to the region $\varepsilon < V, V' < 1$. Equation (29) has different forms in the three areas of possible relations between the external parameters E and ε (i.e., between V_1 and V_k). We write down these three equations in the allowed region $\varepsilon < V, V' < 1$:

(1) Σ_1. For $E + U - \varepsilon < \varepsilon < 1$ [here, the argument of the middle θ function in Eq. (21) is positive]

$$\lambda\varphi(V) = \int_{\varepsilon}^{1} \varphi(V')dV'. \tag{30}$$

(2) Σ_2. For $\varepsilon < E + U - \varepsilon < 1$,

$$\lambda\varphi(V) = \theta(E + U - \varepsilon - V)\int_{E+U-V}^{1} \varphi(V')dV' + \theta(V - E - U + \varepsilon)\int_{\varepsilon}^{1} \varphi(V')dV'. \tag{31}$$

(3) Σ_3. For $\varepsilon < E + U - 1 < 1$,

$$\lambda\varphi(V) = \theta(V - E - U + 1)\int_{E+U-V}^{1} \varphi(V')dV'. \tag{32}$$

We immediately note that the solution in the third area does not contribute to Eq. (26) due to vanishing of the functions $I(\varepsilon_1)$ and $I(\varepsilon_2)$ [Eq. (27)]. Indeed, as follows from the left inequality in the definition of the third area, $1 - U < E - \varepsilon = \min\{V_1, V_k\}$. This contradicts the external constraint (28). Thus, we need to consider only the two remaining areas.

In the first area, Σ_1, Eq. (30) possesses a single solution (the superscript indicates the area):

$$\varphi^{(1)}(V) = \frac{1}{\sqrt{1-\varepsilon}}\theta(V - \varepsilon)\theta(1 - V), \tag{33}$$

$$\lambda^{(1)} = 1 - \varepsilon, \tag{34}$$

which means that the matrix A in this area reduces to a projector. However, the area Σ_1 contributes to the integral (26) only when $U < 1/2$. This becomes obvious if we rewrite the left inequality in the condition defining this area in the form $E + U - \varepsilon = \min\{V_1, V_k\} + U < \varepsilon = \max\{V_1, V_k\}$ and account for the external requirement $\max\{V_1, V_k\} < 1 - U$ (28). For the case $U < 1/2$, the sector $V_1 < V_k$ of Σ_1 is depicted in Fig. 4(a). Integrating in (26) over Σ_1, we find the contribution $P_s^{(1)}$ of this area to the probability P_s:

$$P_s^{(1)} = (1 - U)^N \left(\frac{1 - 2U}{1 - U}\right)^2. \tag{35}$$

In the second area, Σ_2, the eigenfunctions of the integral equation (31) have the following form:

$$\varphi^{(2)}(V) = [A\cos(\mu V) + B\sin(\mu V)]\theta(E + U - \varepsilon - V) + C\theta(V - E - U + \varepsilon). \tag{36}$$

Here, for convenience, the notation μ has been introduced for the inverse eigenvalue

$$\mu = 1/\lambda, \tag{37}$$

so we need to find solutions with the smallest modulus of μ. Equation (31) imposes a set of conditions on the coefficients

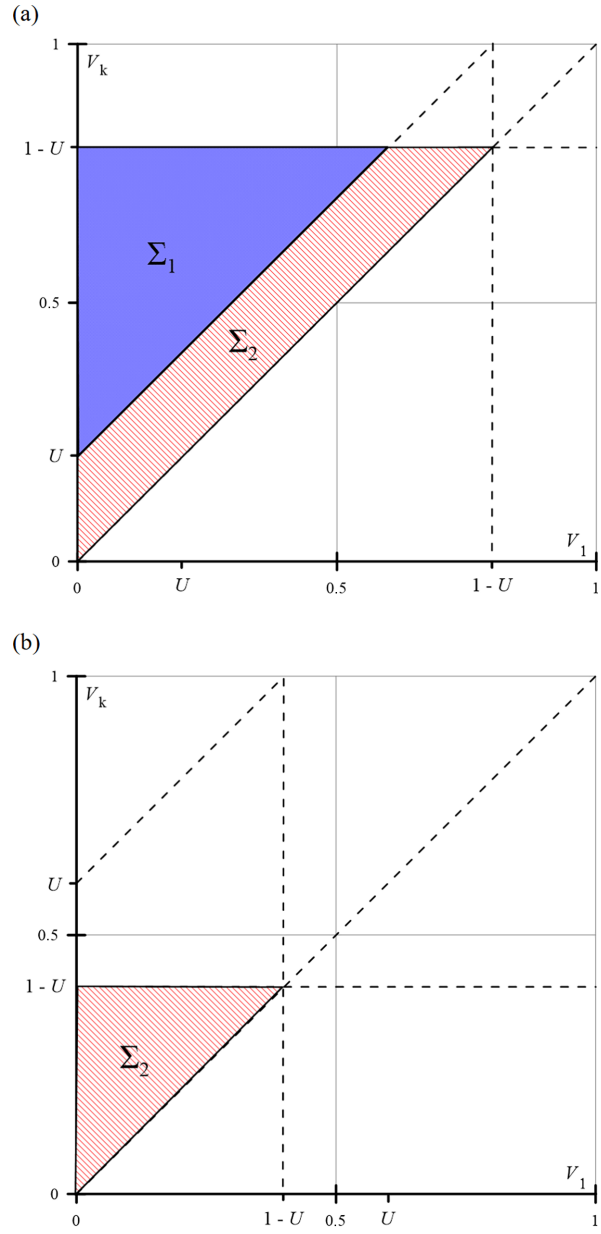

FIG. 4. The areas Σ_1 and Σ_2, determined by the conditions (30) and (31), on the plane of the "external" variables V_1 and V_k (in the sector $V_1 < V_k$) for (a) interaction strength $U < 1/2$ and (b) $U \geqslant 1/2$.

A, B, and C:

$$\begin{aligned} C\mu(1 - E - U + \varepsilon) &= B\cos[(E + U - \varepsilon)\mu] \\ &\quad - A\sin[(E + U - \varepsilon)\mu], \\ A\{1 + \sin[(E + U)\mu]\} &= B\cos[(E + U)\mu], \\ B\{1 - \sin[(E + U)\mu]\} &= A\cos[(E + U)\mu], \\ B\cos(\varepsilon\mu) - A\sin(\varepsilon\mu) &= C, \end{aligned} \tag{38}$$

where the second and third linear equations are equivalent (the determinant of this subsystem is identically zero). System (38) leads to the characteristic equation for μ:

$$(1 - E - U + \varepsilon)\mu = \tan\left(\frac{\pi}{4} - \frac{(E + U - 2\varepsilon)\mu}{2}\right), \tag{39}$$

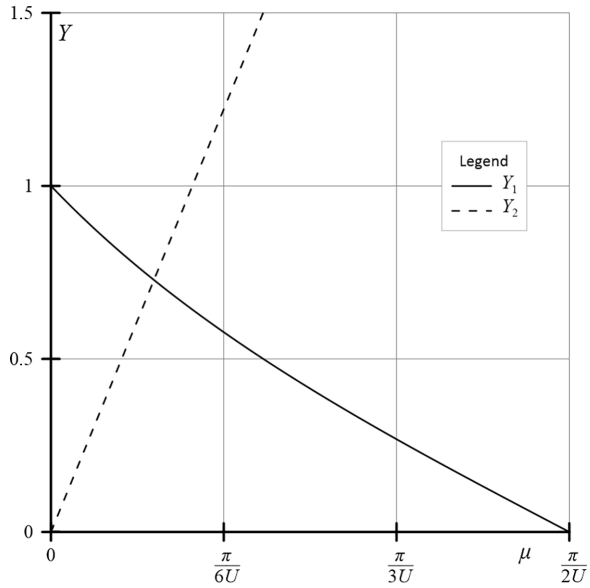

FIG. 5. Graphic representation of the characteristic equation (39). It corresponds to the intersection of the curve $Y_1 = \tan[\pi/4 - \mu(U + V_1 - V_k)/2]$ and the straight line $Y_2 = \mu(1 - U - V_1)$.

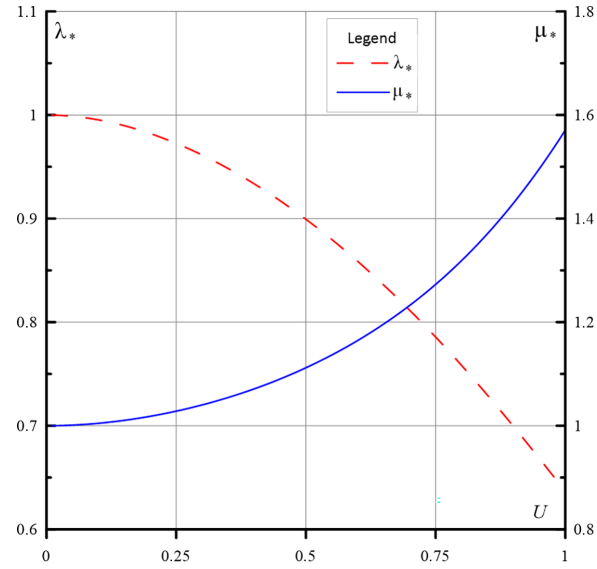

FIG. 6. Dependence of μ_* and $\lambda_* = 1/\mu_*$ on U given by the numerical solution of Eq. (42).

which has an infinite number of solutions for a given set of parameters E, ε, and U. The solution of our interest μ_0 with the minimal modulus lies in the interval where the tangent argument varies between 0 and $\pi/4$ (see Fig. 5).

Coefficients A and B can be expressed via μ_0 and C, with C determined by the normalization condition

$$\int_0^1 \left|\varphi_0^{(2)}(V)\right|^2 dV = 1. \tag{40}$$

Coefficient C also determines the functions $I(\varepsilon_1)$ and $I(\varepsilon_k)$ in Eq. (26). Indeed, both ε_1 and ε_k are greater than $E + U - \varepsilon$; hence, the eigenfunction $\varphi^{(2)}(V)$ in the integrand of Eq. (27) is just C [see Eq. (36)], so

$$I(\varepsilon_1) = (1 - \varepsilon_1)C\,,\ \ I(\varepsilon_k) = (1 - \varepsilon_k)C. \tag{41}$$

Both C and $\mu_0 = 1/\lambda_0^{(2)}$ are functions of U and variables V_1 and V_k within area Σ_2. This area exists for any U (from the interval $0 < U < 1$) and is depicted (for the sector $V_1 < V_k$) in Figs. 4(a) and 4(b) for $U < 1/2$ and $1/2 < U$, respectively.

The transcendental equation (39) for μ can be solved only numerically. In general, this makes a straightforward analytical calculation of the integral (26) over area Σ_2 impossible. However, an analytical calculation is possible in the limit of our interest $N \gg 1$. The leading in N contribution to the integral over Σ_2 is given in the vicinity of the point (V_{1*}, V_{k*}), where $\lambda_0^{(2)}(V_1, V_k)$ has a maximum, i.e., $\mu_0(V_1, V_k)$ is minimal (in modulus).

This minimum μ_* is reached at the point $(V_1 = 0, V_k = 0)$. To prove this statement, we consider, for certainty, the sector $V_1 < V_k$ and note that the value of μ is determined graphically on the plane (μ, Y) by the intersection of the curve $Y_1 = \tan[\pi/4 - \mu(U + V_1 - V_k)/2]$ and the straight line $Y_2 = \mu(1 - U - V_1)$ (Fig. 5). With a fixed slope of the straight line Y_2 (i.e., fixed V_1), the intersection of the curve and the straight line occurs at a smaller coordinate μ the closer the right end of the interval is to the origin. So the minimum occurs at the minimal V_k that corresponds to the case $V_k = V_1$. Further, we note that the smaller the intersection coordinate μ is, the steeper the line Y_2 is. Its steepness increases with the decrease in V_k and becomes maximal at $V_k = 0$. This proves the announced statement that the minimal value μ_* is determined by the numerical solution of the equation

$$(1 - U)\mu = \tan\left(\frac{\pi}{4} - \frac{U\mu}{2}\right). \tag{42}$$

Its solution $\mu_*(U)$, together with $\lambda_*(U) = 1/\mu_*(U)$, is plotted as a function of U in Fig. 6. In the close vicinity of the point $(V_1 = 0, V_k = 0)$ the function $\mu_0(V_1, V_2)$ can be represented as $\mu_0(V_1, V_k) = \mu_* + \delta\mu$, where the leading order correction, determined by Eq. (39), is given by

$$\delta\mu(V_1, V_k) = \gamma_1 V_1 + \gamma_k V_k, \tag{43}$$

$$\gamma_{1(k)} = \frac{1 \mp (1 - U)^2\mu_*^2}{2(1 - U) + U[1 + (1 - U)^2\mu_*^2]}\,; \tag{44}$$

here, the upper (lower) sign relates to γ_1 (γ_k). Correspondingly, the Nth power of the maximal eigenvalue $\lambda_0^{(2)} = 1/(\mu_* + \delta\mu)$ in the vicinity of the point $(V_1 = 0, V_k = 0)$ can be represented as

$$[\lambda_0^{(2)}(V_1, V_k)]^N = \lambda_*^N \exp\left(-\frac{N\delta\mu(V_1, V_k)}{\mu_*}\right), \tag{45}$$

where $\lambda_* = \lambda_0^{(2)}(0, 0) = 1/\mu_*$. As seen from Eq. (45) typical values of $V_1, V_k \sim 1/N \ll 1$, which justifies the linearization of the characteristic equation. This smallness allows us to take the functions $I(\varepsilon_1)$ and $I(\varepsilon_k)$ in the integrand of Eq. (26) at $V_1, V_2 = 0$. Using Eq. (41), we get $I(\varepsilon_1) = I(\varepsilon_k) = C$, where the normalization constant C, determined by Eq. (40) at

$V_1, V_2 = 0$, equals

$$C^2 = \frac{2}{2 - U + U(1-U)^2\mu_*^2}. \tag{46}$$

Performing the integration in Eq. (26) we arrive at the final expression for the contribution $P_s^{(2)}$ from area Σ_2 to the probability P_s:

$$P_s^{(2)}(U) = \frac{2(1-U)^4\lambda_*^{N-2}(U)}{\lambda_*^2(U) + (1-U)^2}[1 - e^{-\gamma_k NU}]. \tag{47}$$

At $1/N \ll U$, the term $\exp(-\gamma_k NU)$ is negligible and can be omitted. We deliberately keep this term for further discussion of the range of ultrasmall $U \ll 1/N$.

Equation (47) holds for almost all values of U, except the narrow region $1 - U \ll 1/N$, in which the domain Σ_2 shrinks to a tiny triangle [see Fig. 4(b)]. In the integral (26) over this triangle we may neglect the dependence of the eigenstate λ_0 on the coordinates, but we have to account for this dependence in function (27): $I(\varepsilon_1) = C(1 - U - V_k)$ and $I(\varepsilon_k) = C(1 - U - V_1)$ [see Eq. (41) in the sector $V_1 < V_k$]. As a result, we obtain

$$P_s^{(2)}(U) = \frac{2N^2}{9}(1-U)^6\lambda_*^{N-4}(U), \quad 1 - U \ll \frac{1}{N}, \tag{48}$$

where $\lambda_*(U = 1) = 2/\pi$.

C. Results and discussion

The expressions (35), (47), and (48) completely determine the probability $P_b(U) = 1 - P_s^{(1)}(U) - P_s^{(2)}(U)$ for two fermions to form a bound pair (i.e., to be localized on neighboring sites) in the ground state of a long, strongly disordered chain. Except in the narrow region $1 - U \ll 1/N$, $P_b(U)$ is given by

$$P_b(U) = 1 - \theta(1/2 - U)(1-U)^N\left(\frac{1-2U}{1-U}\right)^2 - \frac{2(1-U)^4\lambda_*^{N-2}(U)}{\lambda_*^2(U) + (1-U)^2}[1 - e^{-\gamma_k NU}]. \tag{49}$$

The contributions from areas Σ_1 and Σ_2 are mostly determined by the high powers of $1 - U$ and λ_*, respectively. According to the characteristic equation (42), the minimal inverse eigenvalue μ_* obeys the inequality $(1 - U)\mu_* < 1$ (because the tangent function is less than unity at the interval of interest; see Fig. 5). This means $1 - U < \lambda_*$, and at a not too small U the contribution $P_s^{(1)}(U)$ is much smaller than $P_s^{(2)}(U)$; the latter is also small and decreases exponentially with the increase of N. However, both eigenvalues $1 - U$ and $\lambda_*(U) \approx 1 - U^2/2$ tend to unity when $U \ll 1$. As we shall see, the crossover from bound to decoupled fermions occurs just at small $U \ll 1$, so this range deserves particular attention.

As shown in Sec. III A, in the regime of ultralow $U \ll 1/N$, the interaction gives only a tiny correction (14) to the trivial combinatoric expression (3). Both terms are written in the limit of large N and are beyond the accuracy of our subsequent analysis. To illustrate the consistency of the latter, note that "large" linear terms ($\sim NU$) of the formal expansion of the two terms in Eq. (49) mutually cancel. The fermions may be considered to be almost decoupled in this regime.

At larger U, when $1/N \ll U \ll 1/N^{1/4}$, the term $P_s^{(1)} \propto \exp[N\ln(1-U)]$ becomes exponentially small, while the term $P_s^{(2)} \approx \exp(-NU^2/2)$ varies between unity and (almost) zero. The binding probability $P_b(U)$ in this range,

$$P_b(U) = 1 - e^{-NU^2/2}, \tag{50}$$

describes the crossover at

$$U \sim 1/\sqrt{N} \tag{51}$$

from the regime of almost decoupled fermions (at $1/N \ll U \ll 1/N^{1/2}$) to the almost bound ones (at $1/N^{1/2} \ll U$). Note that the calculated functional dependence of $P_b(U)$ in this regime coincides with that obtained with the qualitative reasoning in Sec. III B [see the paragraph above Eq. (15)] and fixes the value of the unknown constant: $\eta^2 = 1/2$.

At still larger values of U both $P_s^{(1)}(U)$ and $P_s^{(2)}(U)$ decay exponentially with the increase of N, so the binding probability P_b approaches unity, while the decoupling of fermions in a long chain becomes a rare event. At $U < 1/2$, the decoupling probability $P_s = P_s^{(1)} + P_s^{(2)}(U)$ is determined by the contributions from both areas Σ_1, (30), and Σ_2, (31); the latter contribution dominates. At $1/2 < U$, the decoupling probability is given entirely by Eq. (47) and is an exponentially decaying function of N: $P_s^{(2)}(U) \propto \exp\{-N\ln[1/\lambda_*(U)]\}$, with $\lambda_*(U)$ changing from ≈ 0.9 to $2/\pi$ when U changes from $1/2$ to 1. At a fixed number of sites, $P_s(U) \propto (1-U)^4 \to 0$ when U approaches unity but still lies outside the narrow region $1 - U \ll 1/N$, where this dependence changes to $P_s(U) \propto N^2(1-U)^6$.

All these analytical results are confirmed by numerical experiments (see Fig. 2).

V. CONCLUSION AND OPEN PROBLEMS

We have described a disorder-induced decoupling of a pair of identical fermions with a short-range attractive interaction on a finite lattice cluster with random on-site energies. In contrast to attracting nonidentical fermions (e.g., with different spins), which can simultaneously occupy a site with minimal energy and thus always form a bound state resistant to disorder, for the identical fermions the probability P_b of pairing on neighboring sites depends on the relation between the interaction $\widetilde{U}$ and the disorder distribution width W (both $\widetilde{U}$ and W are assumed to be large compared to the kinetic energy, i.e., the intersite hopping rate, so the system is deeply in the regime of the single-particle Anderson localization [10]).

For a cluster of arbitrary dimension, we have presented a qualitative argument for a crossover between the regimes of almost coupled and almost decoupled configurations in the ground state. This crossover takes place at $\widetilde{U}/W \sim 1/\sqrt{N}$, where N is the number of lattice sites ($N \gg 1$). However, a straightforward brute-force analytical calculation or computation of the pairing probability P_b as a function of $\widetilde{U}$ and W is an arduous task even for the simplest cluster in the form of a closed chain and for the simplest boxlike distribution of the disorder. The latter problem turns out to be equivalent to the computation of the volume of a polyhedron (in general, NP-hard).

Remarkably, we have found that in the chain geometry the problem can be solved by the transfer matrix method. In the case of the box distribution of the disorder, the eigenvectors and the eigenvalues of the transfer matrix can be derived analytically (another wonder!) from a rather nontrivial integral equation. Using this approach, we have calculated the pairing probability in the long chain for an arbitrary relation between the interaction and the disorder strengths. In particular, we have explicitly described the coupling-decoupling crossover. The obtained results are in agreement with numerical (Monte Carlo) experiments.

In the above analysis we studied the model with zero hopping, thus neglecting the quantum kinetic effects. In general, there may be a drastic difference between the Hubbard models in the limits of zero and small, but nonzero, hopping. This difference takes place for models with spinful electrons and results from a huge spin degeneracy of the ground state at zero hopping, while even a small hopping transfers the half-filled state to an antiferromagnetic state (see, e.g., reviews [15] and [16]). Fortunately, such a singularity is absent for the studied strongly disordered model of spinless fermions in which the weak hopping effects reduce to a little smearing of the particle wave function localized at a given site [10]. It seems plausible that the nonzero, but weak, hopping in such a situation will not have a strong influence on the "classical" model. Certainly, accounting for nonzero hopping will be necessary in studies of dynamical (quantum) properties.

The studied model might have a physical implementation in systems of cold atoms in optical lattices with randomly modulated on-site potentials. Note that as long as we consider only two particles, the model is equally applicable to hard-core bosons. In this paper we have used fermionic terminology, keeping in mind future applications to many-particle systems. Formally, the model can also be mapped on the Ising spin chain in a random magnetic field, but with an unnatural restriction to only two inverted spins sector of the Hilbert space.

The unveiled solvability of the one-dimensional *disordered* model is a kind of serendipity. It is not clear yet whether there is a deeper mathematical reason behind the curtain. At any rate, it would hardly make things trivial: the transcendental equations (39) and (42) for the eigenvalues do not look to be.

It would be interesting to consider the generalization of the present theory to the case of an arbitrary (e.g., Gaussian) distribution of the site disorder $p(V)$ when the transfer matrix is given by Eq. (19) and the possibility of its analytical diagonalization is not *a priori* obvious.

Finally, a generalization of the considered two-particle model (with an effective "filling factor" $2/N$) to a strongly disordered Hubbard-like model with a low, but finite, particle density is an appealing issue for future study.

ACKNOWLEDGMENTS

We thank G. V. Shlyapnikov for discussions at an early stage of this work. V.I.Y. acknowledges the Basic research program of HSE.

[1] N. F. Mott, Adv. Phys. **50**, 865 (2001).
[2] B. L. Altshuler and A. G. Aronov, in *Electron-Electron Interaction in Disordered Systems*, edited by A. L. Efros and M. Pollak (Elsevier, Amsterdam, 1985), p. 1.
[3] P. A. Lee and T. V. Ramakrishnan, Rev. Mod. Phys. **57**, 287 (1985).
[4] V. F. Gantmakher and V. T. Dolgopolov, Phys.-Usp. **53**, 1 (2010).
[5] C. De Dominicis and I. Giardina, *Random Fields and Spin Glasses: A Field Theory Approach* (Cambridge University Press, Cambridge, 2006).
[6] M. Pollak, M. Ortuño, and A. Frydman, *The Electron Glass* (Cambridge University Press, Cambridge, 2013).
[7] I. Bloch, J. Dalibard, and W. Zwerger, Rev. Mod. Phys. **80**, 885 (2008).
[8] B. DeMarco and D. S. Jin, Science **285**, 1703 (1999).
[9] J. Hubbard, Proc. R. Soc. London, Ser. A **276**, 238 (1963).
[10] P. W. Anderson, Phys. Rev. **109**, 1492 (1958).
[11] B. Derrida, Phys. Rev. Lett. **45**, 79 (1980); Phys. Rev. B **24**, 2613 (1981).
[12] H. Ong, H. Huang, and W. Huin, Adv. Eng. Software **34**, 351 (2003).
[13] A. Bhattacharya, K. K. Dubey, and B. Mondal, J. Geom. Graphics **27**, 001 (2023).
[14] H. A. Kramers and G. H. Wannier, Phys. Rev. **60**, 252 (1941).
[15] P. A. Lee, N. Nagaosa, and X.-G. Wen, Rev. Mod. Phys. **78**, 17 (2006).
[16] D. P. Arovas, E. Berg, S. A. Kivelson, and S. Raghu, Annu. Rev. Condens. Matter Phys. **13**, 239 (2022).